International Journal of Thermophysics (2024) 45:8
https://doi.org/10.1007/s10765-023-03294-z

Viscosity, Interfacial Tension, and Density of 2-Propanol and Acetone up to 423 K by Surface Light Scattering and Conventional Methods

Manuel Kerscher[1] · Lena M. Braun[1] · Julius H. Jander[1] · Michael H. Rausch[1] · Thomas M. Koller[1] · Peter Wasserscheid[2,3] · Andreas P. Fröba[1]

Received: 6 November 2023 / Accepted: 8 November 2023 / Published online: 18 December 2023

Abstract

Despite the extensive use of 2-propanol and acetone in a wide range of applications in the chemical industry and in energy engineering, there is a lack of experimental data in the literature for their thermophysical properties including viscosity, interfacial tension, and density, especially at elevated temperatures beyond the respective normal boiling points. In the present study, the liquid viscosity and interfacial tension were determined simultaneously by surface light scattering (SLS) with average expanded uncertainties of (1.7 and 0.9)% at or close to saturation conditions for temperatures between (273 and 403) K. Furthermore, capillary viscometry (CV) and vibrating-tube densimetry were employed to measure the liquid viscosity at ambient pressure of 0.1 MPa from (283 to 353) K and the liquid density close to saturation conditions between (278 and 423) K. The obtained density data were used for the evaluation of both SLS and CV experiments. In comparison with literature data, the present density data show agreement for 2-propanol over the entire temperature range. In contrast, deviations of up to 0.5% at the maximum temperature can be found for acetone. For the viscosity and interfacial tension at low temperatures, agreement of the measurement results among each other and with literature data is mostly found. At elevated temperatures, the increasing deviations of the present experimental viscosity and interfacial tension data from recommended correlations indicate a lack of reliable data needed for their development. Overall, this work contributes to an improvement of the database for viscosity, interfacial tension, and density of 2-propanol and acetone over a wide temperature range up to 423 K.

Keywords Acetone · Density · Interfacial tension · 2-Propanol · Surface light scattering · Thermophysical properties · Viscosity

Extended author information available on the last page of the article

1 Introduction

2-Propanol and acetone represent important bulk chemicals with a wide range of industrial applications. Both are often employed as solvents for various purposes such as reaction, separation, and extraction processes [1–9] or as reaction educts for the production of valuable derivatives [10–15]. In addition to their use as fuel additives [16–19], the pair of 2-propanol and acetone has attained increasing interest in the recent years in the context of direct 2-propanol fuel cells [20–23]. Here, 2-propanol provides several advantageous characteristics with respect to an efficient fuel cell performance [23–25] and, in contrast to the more established direct methanol fuel cell, the complete absence of carbon dioxide formation [26, 27]. Recent developments aim at the operation of direct 2-propanol fuel cells at temperatures of about 373 K [23, 28] and in dilute aqueous solutions of 2-propanol [23] for an improved performance. Moreover, in applications where acetone is hydrogenated to 2-propanol and the resulting 2-propanol is later converted back to acetone and hydrogen (H_2) by the respective dehydrogenation reaction, acetone and 2-propanol act as hydrogen-lean and hydrogen-rich counterparts of a very promising liquid organic hydrogen carrier (LOHC) system that is characterized by excellent reversibility and comparatively low heats of hydrogenation and dehydrogenation [28, 29].

For the design and optimization of the above-mentioned processes and apparatuses in chemical and energy engineering, accurate knowledge of the thermophysical properties of 2-propanol and acetone is required. Despite the extensive use of these two components in many engineering applications, reliable information on their thermophysical properties including viscosity, interfacial tension, and density is only sparsely available in the literature, particularly at temperatures T beyond the respective normal boiling points. This stimulated experimental investigations of the thermophysical properties of pure 2-propanol and acetone in the present study. The results will also serve as a reference for subsequent studies of aqueous solutions with 2-propanol and/or acetone under conditions relevant for the direct 2-propanol fuel cell operation.

In the present work, surface light scattering (SLS) was used to determine simultaneously liquid viscosity and interfacial tension of 2-propanol and acetone at or close to saturation conditions over an extended range of T between (273 and 403) K. Since SLS represents an absolute method without the need for any calibration and is based on a strict theory, it is established as a quasi-primary method for the measurement of viscosity [30, 31]. In addition to SLS experiments, capillary viscometry (CV) was applied at ambient pressure $p = 0.1$ MPa and at T below the normal boiling points of the liquids for comparison purposes. With the help of vibrating-tube densimetry (VTD), the liquid density of both substances was determined at T between (278 and 423) K and at $p = 0.1$ MPa or close to saturation in order to extend the database in the literature and to provide reliable data for the evaluation of the SLS and CV measurements. In the following, the investigated materials and their preparation are described first. Then, the experimental methods, experimental conditions, and uncertainties are briefly stated, before

finally the experimental results of this work for liquid density, interfacial tension, and liquid viscosity are presented and discussed in comparison with literature data.

2 Experimental Section

2.1 Materials and Sample Preparation

Details on the used samples of 2-propanol and acetone as well as on helium (He) employed as inert gas during SLS experiments and argon (Ar) used for sample storage are summarized in Table 1. Therein, information on the molar mass M, the normal boiling point temperature T_b, the critical temperature T_c, and the sample purity are included. The latter is based on the information provided in the certificates of analysis of the providers. Here, the purity of the liquid samples is specified in terms of the peak areas from gas chromatography coupled with flame-ionization detection (GC-FID), whereas that of the gases is provided in terms of mole fractions y. Before investigations, the required amounts of liquid samples were degassed for about 15 min in a glass container immersed in an ultrasound bath at ambient T.

2.2 Vibrating-Tube Densimetry (VTD)—Liquid Density

For the measurement of the liquid density ρ_L of 2-propanol and acetone at T between (278 and 423) K, two instruments from Anton Paar based on the vibrating-tube method were employed. The model DMA 5000 M with a calibrated expanded (coverage factor $k=2$) uncertainty of $U_r(\rho_L)=0.02\%$ [35] and $U(T)=0.01$ K was used to determine ρ_L of 2-propanol at $T\leq 353$ K and that of acetone at $T\leq 323$ K at ambient atmosphere with $p = 0.1$ MPa. For each sample, at least two measurement series were performed with new fillings of the U-tube in between. The corresponding data which always agreed within $\pm 0.008\%$ were then averaged. To cover T above the boiling points of the samples, the model DMA 4200 M with a calibrated uncertainty ($k=2$) of $U_r(\rho_L)=0.1\%$ [36] and $U(T) = 0.03$ K was connected to a temperature-controlled sample reservoir via a short capillary line. In this line, a heated spindle press and a pressure transducer (PAA 33X from Keller) with an expanded ($k=2$) uncertainty of $U(p)=15$ kPa were integrated. This allowed to adjust p to about

Table 1 Specification of the used chemicals

sample	CAS number	source	M/(g·mol^{-1})	T_b/K	T_c/K	specified purity
2-propanol	67-63-0	Sigma Aldrich	60.095	355.5 [32]	508.3 [33]	≥ 0.999[a]
acetone	67-64-1	Sigma Aldrich	58.079	329.22 [34]	508.1 [34]	≥ 0.999[a]
helium	7440-59-7	Air Liquide S.A	4.0026	–	150.69 [34]	$y \geq 0.99999$
argon	7440-37-1	Air Liquide S.A	39.948	–	5.1953 [34]	$y \geq 0.99996$

[a]Purity as specified in the certificate of analysis provided by the supplier, based on peak areas from GC-FID

0.1 MPa for $T \leq T_b$ or a value slightly above the vapor pressure of the sample for $T > T_b$ in order to maintain a slightly compressed liquid phase with a recorded p stability of better than ± 0.4 kPa during a single measurement. With the help of a valve system, the pure samples were filled into the evacuated measurement system. Repetition measurements performed at $T = 298$ K after the highest T of 423 K agreed well with the previous results and, thus, confirm thermal stability of the sample and repeatability of the measurements.

After each measurement with 2-propanol, the water content of the sample was determined by Karl-Fischer titration. On average, a water content of about (1300 and 470) ppm was found for the measurements with the DMA 5000 M at ambient atmosphere with $p = 0.1$ MPa and for the measurements with the DMA 4200 M in the slightly compressed liquid phase, respectively. Similar or lower levels are anticipated for the water contents in the respective acetone samples, where no titration could be performed with the methanol-based reagent. The influence of the measured or assumed water contents is estimated by an ideal mole-based mixing rule considering the molar volumes, where deviations from the values for the pure substances by up to (0.04 and 0.02)% at the largest T are obtained for the measurements at $p = 0.1$ MPa and in the slightly compressed liquid phase, respectively. Those values also apply in the case of acetone under the assumption of similar water contents as for 2-propanol in the corresponding measurements. Consequently, the total uncertainty for ρ_L of the pure samples is conservatively estimated by the sum of the calibrated uncertainty of the instruments and the calculated maximum influence of the water contained in the studied samples. Thus, the relative expanded ($k = 2$) uncertainty is $U_r(\rho_L) = (0.06$ and $0.12)\%$ for measurements at $p = 0.1$ MPa and in the slightly compressed liquid phase.

2.3 Surface Light Scattering (SLS) – Liquid Viscosity and Interfacial Tension

SLS was employed for the simultaneous determination of the liquid viscosity η_L and interfacial tension σ of pure 2-propanol and acetone close to saturation conditions at T between (273 and 403) K. The fundamentals of SLS will be summarized only briefly in the following, while more detailed information on its theoretical principles [37, 38] and experimental realizations for accurate thermophysical property research [39–41] can be found in the cited literature.

The SLS technique relies on the analysis of light which is scattered at the phase boundary between a gas (G) and a liquid (L) phase at macroscopic thermodynamic equilibrium. The scattered light is modulated by the surface fluctuations or waves present at the interface and, thus, contains information about their dynamics. With the help of photon-correlation spectroscopy, time-dependent intensity correlation functions (CFs) are recorded which reflect the dynamics of the surface fluctuations with a defined modulus of the wave vector q. For 2-propanol and acetone in the investigated range of T and q, the normalized CFs $g^{(2)}(\tau)$ as a function of the delay time τ recorded in a heterodyne detection scheme always exhibited an oscillatory behavior associated with propagating surface waves. Such temporal behavior can be described by a damped oscillation according to [38]

$$g^{(2)}(\tau) = a + b \exp\left(-\tau/\tau_C\right) \cos\left(\omega_q \tau - \phi\right), \quad (1)$$

where a and b represent experimental constants related to the coherence properties of the optical system and the ratio between scattered and reference light intensities, while ϕ largely accounts for the deviation of the scattering spectrum from an ideal Lorentzian shape [41]. τ_C and ω_q reflect the dynamics of the surface waves in terms of the characteristic mean lifetime or the inverse of the damping Γ ($\tau_C = \Gamma^{-1}$) and the propagation frequency. For reduced capillary numbers Y between 0.4 and 20 observed in the case of 2-propanol at T between (273 and 343) K, the presence of a non-negligible contribution from the rotational flow in the bulk of the fluid in the CF had to be considered. Here, the recorded signal is described by

$$g^{(2)}(\tau) = a + b \exp\left(-\tau/\tau\right)_C \cos\left(\omega_q \tau - \phi\right) - c \exp\left(-\tau/\tau_0\right), \quad (2)$$

where the third term on the right side of Eq. 2 accounts for the additional signal contribution with its amplitude c. The required information of the characteristic viscous time τ_0 is estimated according to the procedure described in Ref. [42]. In the present case of CFs with an oscillatory behavior, η_L and σ can be determined simultaneously by numerically solving the dispersion equation $D(\eta_L, \eta_G, \rho_L, \rho_G, \sigma, \Gamma, \omega_q, q)$ for surface fluctuations at the gas–liquid interface of simple fluids exhibiting no viscoelastic effects in its complete form [37, 38], where the liquid and gas density ρ_L and ρ_G as well as the gas viscosity η_G are required as input data.

For the investigations, two different sample cells were employed within the experimental setup described in Refs. [43, 44]. An aluminum sample cell was used to particularly cover the T range below ambient T, where additionally measurements at higher T were included for an overlap with experiments performed in a stainless-steel sample cell at T between (303 and 403) K. Since the aluminum sample cell allows to maintain p states below ambient pressure, measurements could be performed under true saturation conditions, i.e., for the pure liquid in coexistence with its saturated vapor. For this purpose, the sample was filled into the evacuated aluminum sample cell and subsequently the cell was closed. To avoid traces of air inside the stainless-steel sample cell designed for measurements at elevated T and p, vacuum was shortly applied to the cell partially filled with sample and thereafter He was added to maintain a pressure slightly larger than ambient p. As will also be shown in the discussion of the results, the influence of the He gas atmosphere on η_L and σ can be safely neglected. Details on the employed aluminum sample cell equipped with two Pt-100 resistant probes with a calibrated uncertainty ($k = 2$) of $U(T) = 15$ mK [39, 45] and the stainless-steel sample cell featuring three Pt-100 probes with $U(T) = 30$ mK [44, 46] are given in the corresponding references. The T stability recorded by the probes was always better than ± 4 mK for the aluminum cell and better than ± 12 mK for the stainless-steel cell. The uncertainty ($k = 2$) in the stated measurement T considering the calibrated uncertainty of the probes, the T stability, and the agreement between the readings of the probes are $U(T) = 20$ mK and $U(T) = 60$ mK for the aluminum and stainless-steel cell, respectively.

For each T, six individual CFs were recorded in transmission direction perpendicular to the vapor/gas–liquid interface at different and relatively large moduli of the

wave vector q, where the influence of instrumental line-broadening effects is typically negligible. The different q were adjusted through the external angles of incidence Θ_E between (2.5 and 3.7)°, with larger Θ_E values being employed at larger T. By performing three pairs of measurements at corresponding angles on either side of the surface normal, possible errors in the alignment are eliminated. The power of the frequency-doubled Nd:YVO_4 laser (Verdi V2 from Coherent) with a wavelength *in vacuo* of $\lambda_0 = 532$ nm irradiating the liquid was limited to 40 mW.

For the determination of η_L and σ via the dispersion relation, the measured values for Γ and ω_q at a given q are combined with reference data for ρ_L, ρ_G, and η_G. In the case of ρ_L, the fit according to Eq. 3 is used based on the present experimental values from this work with uncertainties as stated in Section 2.2. For ρ_G of pure 2-propanol [32] and pure acetone [47] at saturation conditions, the cited equations of state (EoS) with estimated relative uncertainties of $U_r(\rho_G) = 1\%$ were employed. η_G of acetone was calculated from the model of Huber [48] with a specified uncertainty of 5%, while η_G of 2-propanol was estimated with an uncertainty of 10% using the Lucas model [49, 50] considering information for the required critical properties [33]. For the measurements in the presence of He, the gas properties are estimated assuming an ideal behavior of the gas mixtures of He and the vapor of the sample under investigation. Based on the initial partial pressure of He with $p = 0.1$ MPa after closing the cell, its T-dependent pressure is approximated considering the vapor pressure of the sample at the initial T as well as the thermal expansion of the liquid with increasing T. The corresponding ρ_G values for pure He are obtained from the REFPROP database [34] employing the EoS of Ortiz Vega et al. [51]. η_G of the gas mixtures is estimated via the Lucas model, for which the critical properties for 2-propanol [33], acetone [34], and He [34] are used.

The reported values for η_L and σ represent the unweighted average of the results obtained from the individual measurements for a given T. Corresponding expanded ($k = 2$) uncertainties were calculated based on error propagation schemes detailed in Refs. [39, 52] considering the standard deviation of the individual results and the uncertainties of the input data. During the data evaluation of the results for acetone, the possibility of weak line-broadening effects was identified. Here, the combination of relatively small η_L values and relatively large σ values of acetone makes the SLS measurements somewhat more prone to line-broadening effects caused by the instrument-specific uncertainty Δq in the definition of q than it is the case for fluids typically studied with this setup [35, 44, 53]. Although instrumental line-broadening effects were proven to be negligible for other fluids with η_L and σ values similar to acetone, such as benzene [45] and methanol [54], a very conservative estimation of such effects shall be made here for the actual q values probed. Based on theoretical considerations in Ref. [40] for a SLS setup that is nearly identical to the present one, a worst-case estimation results in maximum overpredictions of η_L of acetone by at most 0.7% relative to the value for the identical case with $\Delta q = 0$, while the influence on σ remains far below 0.1% and, thus, negligible. The same considerations have been made for 2-propanol particularly at elevated T, which show that instrumental line-broadening effects increase the measured η_L values by 0.3% or less, while their influence on σ can also be neglected. As a consequence, the final uncertainties for the reported η_L values of acetone in the full T range and of 2-propanol at $T \geq 343$ K

were conservatively extended by adding the estimated worst-case errors induced from the line-broadening effects to the uncertainties from the error propagation calculations. On average, η_L and σ of 2-propanol and acetone could be determined with relative uncertainties ($k=2$) of $U_r(\eta_L)=1.7\%$ and $U_r(\sigma)=0.89\%$.

After measurements at the largest T, repetition measurements were performed at $T=323$ K for the same sample. The agreement of the results for η_L and σ from the repetitions with the initial results at $T=323$ K within their uncertainties confirms the thermal stability of the samples up to $T=403$ K. Thus, the two datasets for η_L and σ at $T=323$ K and the related uncertainties were averaged. The measurement with 2-propanol under a He atmosphere at T between (303 and 403) K was performed twice, where the sample cell was cleaned and refilled with fresh sample in between. Since the results from both series agree always within experimental uncertainties with maximum deviations of 1.7% for η_L and 0.75% for σ, the average of the values for σ and η_L as well as for the related uncertainties was considered. The water content of 2-propanol measured by Karl-Fischer titration after a measurement series was always smaller than 1300 ppm. Due to the highly nonlinear composition-dependent behavior of η_L and σ in mixtures of 2-propanol or acetone with water, a precise quantification of the influence of the measured water contents is difficult, but estimated to be at least one order of magnitude smaller than the corresponding experimental uncertainties of η_L and σ.

2.4 Capillary Viscometry (CV) – Liquid Viscosity

CV was applied to measure the liquid kinematic viscosity ν_L at $p=0.1$ MPa in ambient atmosphere at various T below the respective boiling points of the samples. For this, Ubbelohde capillaries of type 0a for 2-propanol at T between (303 and 353) K and of type 0 for acetone at T between (283 and 323) K were used in a thermostatted water bath. Their calibration constants K and Hagenbach correction factors H were determined from measurements with several reference fluids over an extended range of T. For the capillary 0a, measurements with n-dodecane with a specified purity of ≥ 0.997 based on peak areas from GC-FID at $T=$(293 to 353) K and with the viscosity standard S3 from Anton Paar with certified viscosity values at $T=$(353 to 408) K were performed. For the latter measurements at elevated T, an oil bath as described in Ref. [55] was employed. For the capillary 0, measurements with n-octane with a specified purity of ≥ 0.99 based on peak areas from GC-FID as well as with bi-distilled water at $T=$(293 to 353) K were considered.

The measurement T recorded by a Pt-100 resistance probe with a calibrated uncertainty ($k=2$) of $U(T)=40$ mK close to the capillary showed a stability of better than $\pm$(10 and 20) mK during a flow-time measurement at $T\leq 313$ K and above. Consequently, the overall uncertainty in the reported T is estimated to be $U(T)=$(50 and 60) mK at $T\leq 313$ K and above. At a given state point, five flow-time measurements with a maximum relative deviation of 0.1% from their average were recorded to determine ν_L under consideration of the Hagenbach correction. η_L was calculated for each measurement using $\rho_{L,calc}$ according to Eq. 3 and the individual results were ultimately averaged. The relative expanded ($k=2$) uncertainty of η_L is estimated

considering the uncertainties of K and H of the capillaries, the experimental uncertainty of ρ_L, and the uncertainty of the measurement T.

Repetition measurements at $T = (333$ and $303)$ K for 2-propanol and acetone, respectively, after investigations at the largest T agreed well with the previous measurements with relative deviations within $\pm 0.15\%$. The water content measured by Karl-Fischer titration for 2-propanol after the CV measurement series was about 1700 ppm. The impact of the water content on η_L is difficult to quantify, but is assumed to be considerably smaller than the measurement uncertainties of η_L.

3 Results and Discussion

3.1 Liquid Density

The results for ρ_L of 2-propanol and acetone measured by VTD at $p = 0.1$ MPa in ambient atmosphere and in the slightly compressed liquid phase at p close to the vapor pressure p_{vap} of the corresponding substance are listed in Tables S1 and S2 of the Supporting Information. At T where measurements were performed with both measurement instruments, the results clearly agree within the smaller of the two experimental uncertainties, as can be seen later in Fig. 2. Due to the agreement of the density results and the small differences in p between the measurements in the compressed liquid phase and the measurements at ambient atmosphere, all data for a given substance were used to develop a T-dependent correlation for ρ_L close to saturation conditions according to

$$\rho_{L,calc} = \sum_{i=0}^{3} \rho_i \cdot T^i, \tag{3}$$

where the same statistical weight was applied for each data point in the fit by a least-squares minimization algorithm. The obtained fit parameters ρ_i for 2-propanol and acetone describing the experimental data within their uncertainties are listed in Table 2 together with the related average absolute relative deviation (AARD) of the experimental data from their fit.

The experimental results for ρ_L are depicted in Fig. 1 as a function of T together with their fits according to Eq. 3 as well as calculated values for ρ_L at saturation conditions based on the EoS for 2-propanol developed by Scalabrin and Stringari [32] and that for acetone developed by Lemmon and Span [47]. For both fluids, ρ_L shows

Table 2 Parameters of Eq. 3 for the calculation of the liquid density $\rho_{L,calc}$ of 2-propanol and acetone based on VTD data at T between (278 and 423) K

sample	ρ_0/(kg·m^{-3})	ρ_1/(kg·m^{-3}·K^{-1})	ρ_2/(kg·m^{-3}·K^{-2})	ρ_3/(kg·m^{-3}·K^{-3})	AARD[a]/%
2-propanol	1161.73	− 2.5804	7.2987×10^{-3}	-9.8196×10^{-6}	0.006
acetone	1330.31	− 3.3220	7.7142×10^{-3}	-9.1054×10^{-6}	0.013

[a]Average absolute relative deviation of measured ρ_L data from their fit

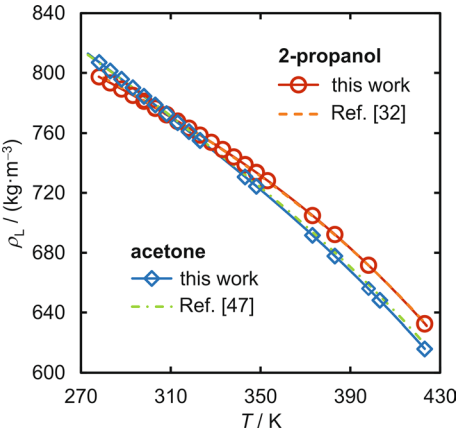

Fig. 1 Liquid density ρ_L of 2-propanol and acetone measured by VTD at $p = 0.1$ MPa under ambient atmosphere or in the slightly compressed liquid phase at p close to p_{sat} as a function of T. For comparison, ρ_L data calculated via the recommended EoS from the literature for 2-propanol [32] and acetone [47] at saturation conditions are included

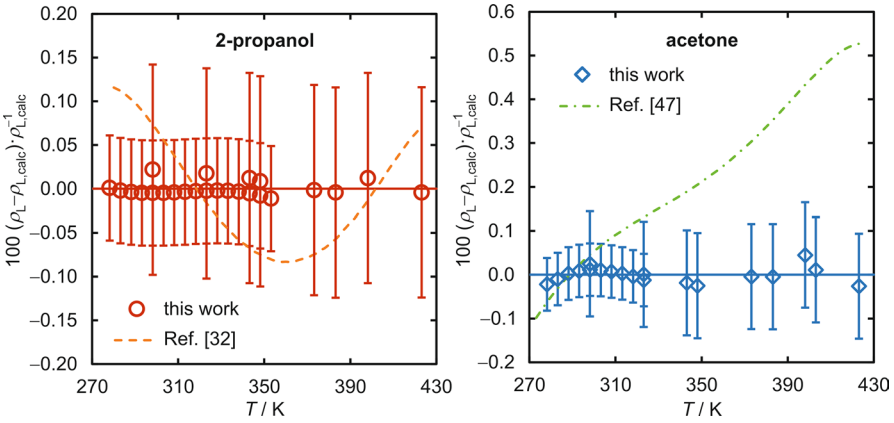

Fig. 2 Relative deviations of measured ρ_L data from their fit according to Eq. 3 as a function of T for 2-propanol (left) and acetone (right). For comparison, corresponding relative deviations of ρ_L data calculated via the recommended EoS in the literature for 2-propanol [32] and acetone [47] at saturation conditions are included

a highly nonlinear T-dependent trend, where for acetone a larger relative decrease of 21% from $T = (278$ to $423)$ K is observed than for 2-propanol with a decrease of 19%. While acetone exhibits a 0.4% larger value at $T = 278$ K than 2-propanol, an increase in T leads to a crossing of the ρ_L data, resulting in a 2.7% smaller value for acetone compared to 2-propanol at $T = 423$ K. The EoS-based literature values for 2-propanol [32] and acetone [47] exhibit generally the same T-dependent behavior as the present results.

For a more detailed comparison of the calculated values obtained from the literature [32, 47] with the present results, their relative deviations from the fit of the experimental data according to Eq. 3 are depicted in Fig. 2 for 2-propanol (left) and acetone (right). Since the works of Scalabrin and Stringari [32] and Lemmon and Span [47] provide an extensive comparison of their EoS with available experimental ρ_L data from the literature, the present discussion is limited to a direct comparison

with the EoS-based values. For 2-propanol, the relative deviations of the literature values with unspecified uncertainties from $\rho_{L,calc}$ remain within about $\pm 0.1\%$ and, thus, agree with the present data within the larger experimental uncertainties of the DMA 4200 M. In the case of acetone on the right side of Fig. 2, the calculated values for ρ_L at saturation conditions show deviations from $\rho_{L,calc}$ within $\pm 0.1\%$ only for T below 313 K, while beyond that T, the deviations increase to $+0.53\%$ at $T=423$ K. This somewhat different T-dependent trend may be related to the limited amount of experimental data for ρ_L of acetone at or close to saturation conditions at $T>320$ K as well as the high scatter among the few available datasets as stated by Lemmon and Span [47], which affects the reliability of the EoS for ρ_L at elevated T. Although not clearly specified in Ref. [47], the REFPROP database [34] states relative uncertainties ($k=2$) for ρ_L of acetone at saturation conditions of $U_r(\rho_L)=0.1\%$ for T between (280 and 310) K, 0.5% for T up to 380 K, and 1% above, which accounts for the lack of accurate experimental ρ_L data in the literature. These uncertainties are always clearly larger than the relative deviations from the present data given on the right side of Fig. 2. The present data may provide a valuable support for a further improvement of the EoS of both substances, which can also reduce the uncertainties related to the calculated ρ_L values of acetone under saturation conditions at T above its normal boiling point.

3.2 Interfacial Tension

The results for the interfacial tension σ of 2-propanol and acetone determined by SLS at saturation conditions and in the presence of a He atmosphere at $p \approx 0.1$ MPa as a function of T are listed in Tables 3 and 4 together with simultaneously determined values for η_L.

For 2-propanol, the σ results obtained in the presence of a He atmosphere at $T=$(303 and 343) K deviate by ($-$ 0.34 and $+0.05$)% from corresponding results obtained in the measurement series under true saturation conditions. For acetone, the σ values obtained in the presence of He at $T=$(323 and 363) K show relative deviations of – (0.57 and 0.87)% from the corresponding results under saturation conditions. The relatively small differences within experimental uncertainties and, in the case of acetone at $T=363$ K, within combined uncertainties indicate a negligible influence of the different atmospheres on the present SLS results for σ. Thus, all σ data listed in Tables 3 and 4 have been considered, where the results at a corresponding T were averaged before fitting. As a result, a T-dependent representation of σ of 2-propanol or acetone by fit according to

$$\sigma_{calc} = \sigma_0 + \sigma_1 \cdot T + \sigma_2 \cdot T^2 \tag{4}$$

is suggested, where each data point was treated with the same statistical weight. The fit parameters σ_0, σ_1, and σ_2 of Eq. 4 obtained by a least-squares minimization algorithm are given in Table 5 together with the AARD of the measured data from σ_{calc}. In all cases, Eq. 4 describes the experimental results for 2-propanol and acetone within their uncertainties.

Table 3 Interfacial tension σ and liquid dynamic viscosity η_L of pure 2-propanol and acetone at saturation conditions determined by SLS as a function of T. In addition, the values for ρ_L, ρ_G, and η_G used for data evaluation are included[a]

T / K	ρ_L/(kg·m^{-3})	ρ_G/(kg·m^{-3})	η_G/(μPa·s)	η_L/(mPa·s)	100 $U_r(\eta_L)$	σ /(mN·m^{-1})	100 $U_r(\sigma)$
2-propanol							
273.15	801.36	0.0234	6.75	4.625	1.6	22.34	1.6
283.15	793.36	0.0555	7.00	3.371	1.9	21.68	1.9
293.16	785.15	0.1049	7.25	2.410	1.7	20.89	1.7
303.16	776.68	0.1887	7.49	1.780	1.5	20.12	1.1
343.14	738.97	1.205	8.48	0.6419	1.7	16.55	1.0
acetone							
273.16	812.89	0.2415	6.92	0.4079	1.8	25.41	0.53
283.16	801.44	0.3875	7.16	0.3640	1.9	24.176	0.36
293.16	790.00	0.601	7.41	0.3330	1.4	22.94	0.59
303.15	778.51	0.901	7.65	0.2998	1.7	21.61	0.58
323.17	755.08	1.857	8.15	0.2467	1.8	19.25	0.87
363.17	705.16	6.09	9.17	0.1768	1.9	14.474	0.47

[a] The sources and calculations of the input data ρ_L, ρ_G, and η_G as well as their relative uncertainties are specified in Section 2.3. The uncertainty for T is $U(T)=20$ mK. All uncertainties are given on a confidence level of 0.95

The experimental σ results for 2-propanol and acetone as well as their corresponding fits σ_{calc} are displayed as a function of T in Fig. 3. Therein, also recommended

Table 4 Interfacial tension σ and liquid dynamic viscosity η_L of 2-propanol and acetone determined by SLS in the presence of a He atmosphere as a function of T. In addition, the values for ρ_L, ρ_G, and η_G used for data evaluation are included

T/K	ρ_L/(kg·m^{-3})	ρ_G/(kg·m^{-3})	η_G/(μPa·s)	η_L/(mPa·s)	100 $U_r(\eta_L)$	σ/(mN·m^{-1})	100 $U_r(\sigma)$
2-propanol							
303.15	776.69	0.338	16.8	1.783	2.2	20.05	1.6
323.18	758.68	0.69	16.8	1.017	1.3	18.33	0.99
343.18	738.93	1.48	15.4	0.6329	1.1	16.558	0.45
363.14	716.97	3.03	13.8	0.4232	1.3	14.654	0.78
383.12	692.28	5.9	12.7	0.2972	1.8	12.689	0.49
403.13	664.36	10.6	12.2	0.2183	1.9	10.561	0.80
acetone							
323.17	755.08	1.66	11.8	0.2438	1.6	19.14	1.1
343.17	730.79	3.59	11.8	0.2069	2.0	16.770	0.52
363.17	705.16	6.16	10.8	0.1743	1.7	14.348	0.40
383.18	677.76	10.1	10.9	0.1500	2.1	12.04	0.97
403.09	648.31	16.0	11.1	0.1280	2.0	9.758	0.50

[a]The sources and calculations of the input data ρ_L, ρ_G, and η_G as well as their relative uncertainties are specified in Sect. 2.3The uncertainty for T is $U(T)=60$ mK. All uncertainties are given on a confidence level of 0.95

Table 5 Coefficients of Eq. 4 for the calculation of σ_{calc} based on SLS measurements at T between (273 and 403) K

substance	σ_0/(mN·m^{-1})	σ_1/(mN·m^{-1}·K^{-1})	σ_2/(mN·m^{-1}·K^{-2})	AARD[a]/%
acetone	64.342	-1.5719×10^{-1}	5.3998×10^{-5}	0.10
2-propanol	32.923	-2.9600×10^{-3}	-1.3026×10^{-4}	0.14

[a]Average absolute relative deviation of measured σ data from their fit

correlations for 2-propanol [56] and acetone [57] from the literature are included for comparison purposes. Based on the SLS results, σ of acetone at $T = 273$ K is 14% larger than that of 2-propanol, while at $T = 403$ K, a 7.6% smaller value is observed. The distinctly different T-dependent trends in σ of both substances, with an intersection of the interfacial tensions at $T \approx 343$ K, are presumably related to different T-dependent influences of the hydroxyl group in 2-propanol and the carbonyl group in acetone on σ in the structurally similar molecules. For acetone, the recommended correlation [57] exhibits the same T-dependent behavior as the SLS data, with generally slightly larger values. For 2-propanol, the recommended correlation by Mulero et al. [56] shows similar values as the present experimental data at low T, while the values increasingly deviate from the SLS results with increasing T. Thus, the correlation for 2-propanol also exhibits strongly increasing deviations from that of acetone at larger T, although the difference in the critical temperature T_c of both substances is only 0.2 K [33, 34]. Since T_c is in fact considered in both correlations such that $\sigma = 0$ at the critical point, they show a converging trend when approaching T_c despite the largely diverging trends in the elevated T range covered by Fig. 3.

For a more detailed discussion of the SLS results and the recommended correlations [56, 57], Fig. 4 displays their relative deviations from the fit according to Eq. 4 for 2-propanol (left) and acetone (right). Experimental data sets for σ of 2-propanol and acetone available in the literature are additionally included. Due to the relatively large amount of experimental studies for σ of the two substances and to ensure

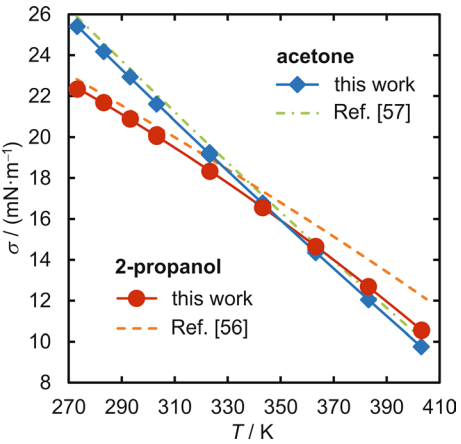

Fig. 3 Interfacial tension σ of 2-propanol and acetone at or close to saturation conditions measured by SLS as a function of T. In addition, recommended correlations for σ of 2-propanol [56] and acetone [57] from the literature are included

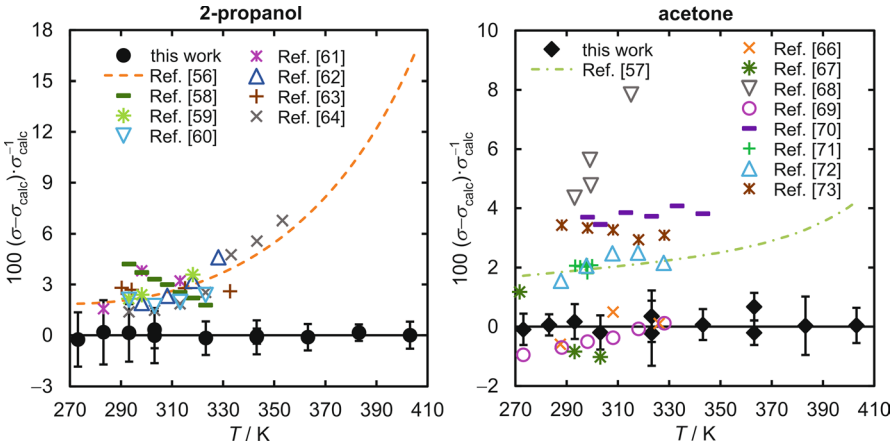

Fig. 4 Relative deviation of measured σ data from their fit according to Eq. 4 as a function of T for 2-propanol (left) and acetone (right). For comparison, also relative deviations of the corresponding recommended correlations [56, 57] as well as experimental literature data for 2-propanol [58–64] and acetone [66–73] as described in the text are depicted

legibility, only data sets from the accessible literature have been considered where measurements for at least three different T are reported.

For 2-propanol discussed in the following, the data from Vazquez et al. [58], Azizian et al. [59], Kao and Tu [60], Andreatta et al. [61], and Chang et al. [62] were obtained by detachment methods using a ring or plate geometry. Vogel [63] employed the capillary rise method, while Ghahremani et al. [64] derived their results from the dynamics of externally generated, macroscopic surface waves. The data from Chang et al. [62] appear to be in parts identical with previously published data from their group obtained with the same apparatus and, thus, only the cited work covering the largest T range is included here. All considered literature data for 2-propanol were presumably measured at ambient atmosphere. As can be seen in Fig. 4, the corresponding data covering T between in total (283 and 353) K generally exhibit slightly larger σ values than the SLS data with relative deviations mostly within about 3% up to $T = 323$ K. With increasing T, the literature data show increasing deviations from the SLS data between 2.6% for the result from Vogel [63] at $T = 333$ K and 6.8% for the result from Ghahremani et al. [64] at $T = 353$ K. The increasing deviations at elevated T may be related to the fact that the measurements in literature were carried out in instruments that are open to the surrounding air atmosphere. This situation leads to considerably different compositions of the contacting gas phase compared to the scenario with a fully saturated vapor atmosphere, as given in the SLS experiments. For instance, it was demonstrated for water that the measurement results for σ at a given T show increasing positive deviations from the reference value at saturation conditions with decreasing relative humidity of the gas phase in contact with the studied liquid [65]. Furthermore, the increasing evaporation rates with increasing T in an unsaturated atmosphere may have a considerable influence on the actual T of the probed interface, resulting in somewhat lower T than the stated values. For example, in the experiments performed by Ghahremani

et al. [64], a petri dish allowing for a relatively large gas–liquid interface was used. Thus, the increasing positive deviations of their σ data from the present SLS data obtained in a closed sample cell under equilibrium conditions seem reasonable when T approaches the boiling temperature $T_b \approx 355$ K of 2-propanol [32]. The correlation by Mulero et al. [56] with unspecified uncertainty follows the T-dependent behavior of the experimental literature values and shows relative deviations from Eq. 4 in the range of + (1.9 to 3.3)% between T = (273 and 323) K which increase up to + 16% at T = 403 K. For the development of their correlation specified for T between (223 and 473) K, Mulero et al. [56] have considered not only the datasets from Azizian et al. [59], Kao and Tu [60], and Andreatta et al. [61], but also further experimental data which are obtained at single T of 298 K. For T below 283 K and above 323 K, the correlation is presumably solely based on databases where it is difficult to identify the origin of the underlying data. Overall, it is obvious that there is a clear lack of reliable and accessible experimental data at elevated T, which seems to be reason for the large discrepancy between the correlation by Mulero et al. [56] and the present SLS results.

In the case of acetone, the experimental literature values for σ displayed on the right side of Fig. 4 originate from eight accessible sources which report data at three or more T points and extend over a T range from (272 to 343) K. Worley [66], Tonomura and Chujo [67], and Cowan et al. [68] employed the capillary rise method, Morgan and Scarlett [69] used the drop-weight method, and Toryanik and Pogrebnyak [70] as well as Stairs et al. [71] applied the maximum bubble-pressure method. The data from Kahl et al. [72] and Enders et al. [73] are based on individual pendant-drop measurements performed with the help of the same experimental setup in a closed sample cell at p = 0.1 MPa in the presence of air saturated with acetone vapor. Comparable conditions are also anticipated for the work of Toryanik and Pogrebnyak [70]. Tonomura and Chujo [67] realized experiments with acetone in its vapor–liquid equilibrium, whereas all other studies were presumably carried out in the presence of ambient air atmosphere. Overall, the deviations of the literature data from σ_{calc} according to Eq. 4 range from (− 1 to + 8)%. Excluding the data from Cowan et al. [68] showing by far the largest deviations, all other data sources deviate by less than about ± 4% from the present results. Here, the data from Worley [66], Morgan and Scarlett [69], and Tonomura and Chujo [67] show very good agreement with the present results within about ± 1%, while the other data exhibit slightly larger positive deviations from σ_{calc}. The values of the recommended correlation for σ of acetone from Mulero et al. [57] are slightly larger than σ_{calc} and increase with increasing T, with relative deviations of + (1.7 and 4.2)% at T = (273 and 403) K. Since the authors only specify the used thermophysical property databases covering T between (182 and 353) K for the development of the correlation, it is unclear whether some of the literature data displayed here are considered therein.

In summary, there is a clear lack of reliable experimental data for σ of 2-propanol and acetone at T close to and above their respective normal boiling points. Since the present SLS investigations at T between (273 and 403) K were conducted in macroscopic thermodynamic equilibrium at or close to true saturation conditions, they provide a valuable and accurate database for the interfacial tension of 2-propanol and acetone up to elevated temperatures.

3.3 Liquid Dynamic Viscosity

The results for η_L of 2-propanol and acetone determined by SLS at saturation conditions and in the presence of a He atmosphere at $p \approx 0.1$ MPa measured by SLS at T between (273 and 403) K are summarized in Tables 3 and 4. Additional data for η_L of both substances measured by capillary viscometry (CV) at ambient atmosphere and $p = 0.1$ MPa at varying T below the respective boiling points are listed in Table S3 of the Supporting Information.

The SLS results obtained for η_L of 2-propanol in the presence of a He atmosphere at $T = (303$ and $343)$ K deviate by $(+0.11$ and $-1.4)\%$ from the values obtained at the same T at vapor–liquid equilibrium. For acetone, the corresponding relative deviations at $T = (323$ and $363)$ K are $-(1.2$ and $1.4)\%$. All deviations agree within the stated individual experimental uncertainties, with the exception of the results for acetone at $T = 323$ K, where agreement at least within combined uncertainties is found. Thus, in a similar manner as performed for the σ data, the individual measurement series obtained in different atmospheres are combined to one data set by forming the unweighted average at overlapping T. The final T-dependent fit correlation $\eta_{L,calc}$ according to

$$\eta_{L,calc} = \eta_0 \cdot \exp\left(\sum_{i=1}^{n} \eta_i \cdot T^{-i}\right) \tag{5}$$

requires more fit parameters for 2-propanol with $n = 4$ than for acetone with $n = 2$ due to the large η_L range covered for 2-propanol. For fitting by a least-squares minimization algorithm, the data were represented by $\ln(\eta_L$ / mPa·s) *versus* T^{-1}/K^{-1}. The resulting fit parameters η_i for 2-propanol and acetone are listed in Table 6 together with the AARD of the experimental values from their fit. For all T, the experimental data are captured by Eq. 5 within their uncertainties.

Starting with 2-propanol first, the corresponding SLS results for η_L including $\eta_{L,calc}$ according to Eq. 5 are displayed as a function of T in the upper part of Fig. 5 together with the CV data measured in this work. To the best of the authors' knowledge, there is no reference correlation or estimation model for η_L of 2-propanol available in the literature. η_L of 2-propanol decreases strongly with increasing T from 4.6 mPa·s at $T = 273$ K to 0.22 mPa·s at $T = 403$ K, which corresponds to a factor of 21. Such a large decrease is presumably related to the distinct weakening of hydrogen bonds present in liquid 2-propanol.

Table 6 Coefficients of Eq. 5 for the calculation of $\eta_{L,calc}$ based on SLS measurements at T between (273 and 403) K

substance	η_0/(mPa·s)	η_1/(K)	η_2/(K^2)	η_3/(K^3)	η_4/(K^4)	AARD[a]/%
acetone	2.77331×10^{-3}	1.93275×10^{3}	-1.55691×10^{5}	–	–	0.44
2-propanol	1.23842×10^{-16}	4.37443×10^{4}	-2.17822×10^{7}	5.03956×10^{9}	-4.30435×10^{11}	0.31

[a]Average absolute relative deviation of measured η_L data from their fit

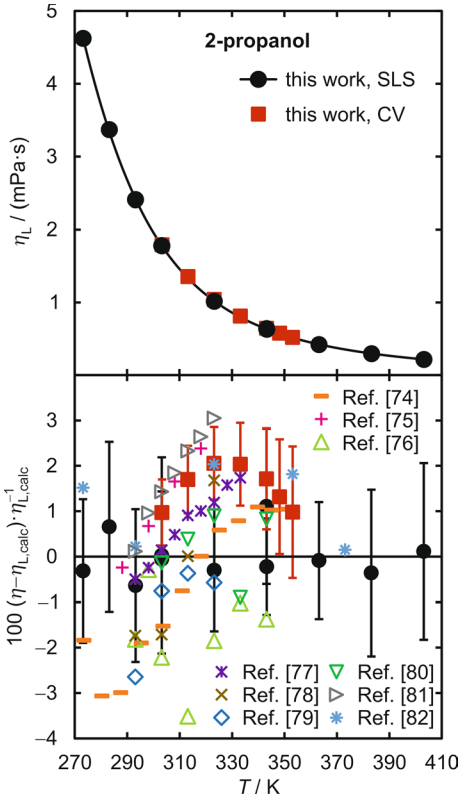

Fig. 5 Liquid dynamic viscosity η_L of 2-propanol measured by SLS at or close to saturation conditions and by CV at $p = 0.1$ MPa under ambient atmosphere (upper part) and its relative deviation from $\eta_{L,calc}$ according to Eq. (5) based on SLS data (lower part) as a function of T. In the lower part, also experimental data from the literature [74–82] as described in the text are included

The lower part of Fig. 5 shows the relative deviations of the SLS and CV data from this work as well as of the experimental literature values for η_L of 2-propanol from $\eta_{L,calc}$. For legibility purposes, only studies where at least four measurements at different T covering a range of 30 K or more are reported have been considered out of the relatively large amount of experimental works reporting η_L data. The data from Thorpe and Rodger [74], Aznarez et al. [75], Yang et al. [76], Pang et al. [77], Awwad et al. [78], Kermanpour and Sharifi [79], and Mesquita et al. [80] are all based on CV measurements, while Shirazi and Kermanpour [81] employed a Stabinger-type rotational viscometer. All these measurements are associated with conditions of ambient air atmosphere. In addition to CV experiments at ambient atmosphere, Weber [82] used also a falling-sphere viscometer to obtain n_L of 2-propanol at $T = 373$ K above its normal boiling point by ensuring a pressure close to the vapor pressure of the pure substance.

The relative deviations of the CV data from this work as well as of the literature values from $\eta_{L,calc}$ displayed in the lower part of Fig. 5 cover a range between (− 3.5 and + 3.1)%. Here, the result from Kermanpour and Sharifi [79] at $T = 333$ K with a relative deviation of − 22% from $\eta_{L,calc}$ was discarded. The CV data from the present work are somewhat larger than the SLS data with a maximum deviation of + 2.1% at $T = 323$ K. Only for this state, the relative deviation is slightly outside combined experimental uncertainties, while agreement within combined uncertainties is given

for all other state points. The data from Thorpe and Rodger [74], Aznarez et al. [75], Pang et al. [77], Awwad et al. [78], and Shirazi and Kermanpour [81] exhibit a slightly different T-dependent behavior compared to $\eta_{L,calc}$. In contrast, the results from Yang et al. [76], Kermanpour and Sharifi [79] excluding their reported value at 323 K, and Mesquita et al. [80] are by trend in accordance with the T-dependent trend of the SLS data. The data from Weber [82] are in better agreement with the present CV data in the intermediate T range, but converge close to $\eta_{L,calc}$ at $T = 373$ K. At this particular state, the falling-sphere apparatus employed by Weber [82] allows for measurements in a closed system similar to the conditions given in SLS experiments, while his CV measurements at lower T may be prone to influences from evaporation effects as well as water absorbed from ambient air. Similar effects may also play a role for the other literature data as well as the CV results from this work, and give a possible explanation for the typically slightly different T-dependent trends in comparison to the SLS data. However, such interpretations are very speculative in view of the overall small relative deviations of the present CV data and further η_L data in literature from $\eta_{L,calc}$ being mostly within $\pm 2\%$.

In the case of acetone, the SLS data for η_L and the related fit according to Eq. 5 are depicted in the upper part of Fig. 6 in combination with corresponding CV data measured in this work as a function of T. This figure also includes calculated values for η_L of acetone at saturation conditions based on the estimation model from Huber [48], which is implemented in the REFPROP database [34] and has a specified uncertainty of 5% along the saturation line. Compared to 2-propanol, η_L of acetone covers a considerably smaller range from (0.41 to 0.13) mPa·s at T from (273 to 403), which is apparently related to the absence of hydrogen bonding interactions between acetone molecules.

The lower part of Fig. 6 shows the relative deviations of the present experimental η_L data, of the estimation model [48], and of experimental data from the literature from $\eta_{L,calc}$ of acetone. Similar as for 2-propanol, the vast amount of accessible studies containing data for η_L is reduced by limiting to those reporting at least three data points covering a T range of 15 K or more. Among these, the data from Faust [91] are excluded due to significant inconsistencies within their own results. While Sih et al. [90] have employed a falling-body viscometer, where no details about the atmosphere in the closed system are specified, all other studies considered here are based on CV measurements at ambient atmosphere [74, 83–89]. The estimation model of Huber [48], for which among the displayed data only those of Yang et al. [89] were considered, shows good agreement with the SLS data at low T within 2% below about 323 K. With increasing T, the model shows increasing positive relative deviations up to 7.5% at $T = 403$ K. As it is evident from the displayed experimental data from the literature, there is a lack of η_L values for acetone at or close to saturation conditions above its normal boiling point ($T_b = 329$ K). At T above T_b, the estimation model mainly relies on η_L data obtained in the compressed liquid phase. Therefore, the displayed calculated values are obtained from extrapolations to the saturation pressure, which induces an additional uncertainty and may explain the increasing deviations from $\eta_{L,calc}$ with increasing T. The experimental literature data for η_L of acetone at $p = 0.1$ MPa exhibit relative deviations between $(-4.8$ and $+10.5)\%$ from $\eta_{L,calc}$, which represents a clearly larger scatter for the

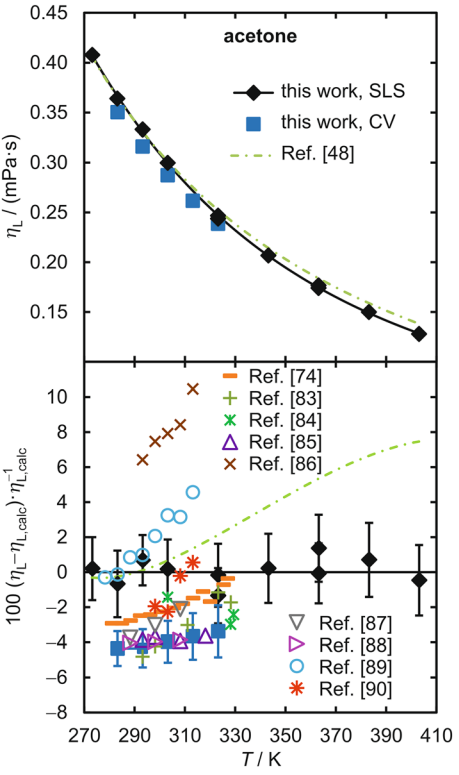

Fig. 6 Liquid dynamic viscosity η_L of acetone measured by SLS at or close to saturation conditions and by CV at $p = 0.1$ MPa under ambient atmosphere as well as calculated values for η_L of acetone at saturation conditions based on the estimation model by Huber [48] as a function of T (upper part). Their relative deviations from $\eta_{L,calc}$ according to Eq. (5) based on SLS data including experimental data from the literature [74, 83–90] as described in the text as a function of T (lower part)

η_L data of acetone compared to 2-propanol. The upper positive boundary is mainly related to the data from Govindarajan et al. [86] which clearly do not agree with any other data set. Excluding the data from Govindarajan et al. [86], the maximum positive deviation from the SLS values is 4.6%. Here, the present SLS results lie rather in the upper band within the range spanned by the remaining datasets, while the CV results from this work mostly mark the lower end of this range. The latter results show relative deviations of around − 4% from $\eta_{L,calc}$ based on the SLS data which are mostly outside combined uncertainties, except for the data at $T = 323$ K. Despite a diligent analysis of the SLS and CV results, possible reasons for the discrepancy remain unclear. Agreement with the SLS results is given in parts with respect to the data from Yang et al. [89] with deviations smaller than ± 1% at T between (278 and 293) K as well as the results from Sih et al. [90] within about ± 2% at $T = (298$ and 303) K and within ± 0.5% at $T = (308$ and 313) K. The data of Thorpe and Rodger [74], Howard and McAllister [83] as well as Peng and Tu [87] exhibit better agreement with the present CV data at low T, but tend toward the SLS results with increasing T. Moreover, the datasets from Hafez and Hartland [85] as well as Chen and Tu [88] agree well with the present CV data. This data comparison reflects the somewhat unsatisfying data situation in the literature for η_L of acetone, as it was also stated by Huber [48]. For this, fluid-specific challenges in the sample handling may be responsible, but also the effects of the measurement principle and/or conditions.

This involves, e.g., the application of a shear gradient in conventional viscometers and/or the presence of a contacting air atmosphere in open viscometers. Such effects are at least excluded for the present SLS investigations because they are conducted in macroscopic thermodynamic equilibrium at or close to saturation conditions.

Overall, the identified lack of experimental data for η_L of 2-propanol and acetone at or close to saturation conditions, especially at T beyond the respective boiling points, could be met by corresponding SLS experiments in the present work. The obtained accurate results for the saturated liquid viscosity over a wide range of T up to 403 K are considered to substantially extend the current data situation for these two pure substances.

4 Conclusions

The present experimental study provides reliable and accurate data for the liquid dynamic viscosity η_L, interfacial tension σ, and liquid density ρ_L of 2-propanol and acetone over a broad T range between (273 and 423) K. Data for ρ_L at T between (278 and 423) K were obtained by VTD at atmospheric pressure or in the compressed liquid phase at p slightly above p_{vap}. The density results for 2-propanol agree well with an available EoS [32], while relative deviations of up to 0.5% at the maximum T between the recommended values [47] and the present experimental data can be found for acetone. The latter behavior is probably related to the sparse amount of reliable ρ_L data at elevated T at or close to saturation conditions which were available for the development of the EoS.

For conditions at or close to saturation, the SLS technique allowed for a simultaneous determination of η_L and σ with typical expanded uncertainties below (2 and 1)% at T between (273 and 403) K. With respect to the interfacial tension, the SLS results for 2-propanol are generally slightly smaller than the values from the accessible literature with deviations mostly within 4%, while the data for acetone obtained by SLS lie in the lower band of the somewhat scattered values in the literature and agree with most data sets within about 3%. The increasing positive deviations of the recommended reference correlations for σ of both substances [56, 57] from the SLS results with increasing T appear to be related to a lack of reliable experimental data at T above the normal boiling point. For comparison purposes, additional viscosity measurements were performed by CV at temperatures below T_b and at ambient atmosphere. For 2-propanol, the η_L data from SLS agree with the CV results and with most of the literature data within $\pm 2\%$. In the case of acetone, the larger relative deviations of about 4% between the present SLS and CV data, which are mostly outside combined uncertainties, together with the relatively large scatter among corresponding viscosity values reported in the literature of up to 15% might indicate difficulties in the accurate measurement of η_L for the low-viscosity fluid acetone. η_L of acetone at saturation conditions calculated with REFPROP [34, 48] exhibits increasing deviations from the present experimental data with increasing T above the normal boiling point, which might again reflect the scarce data situation in the literature at elevated T.

In summary, the present experimental data for ρ_L, σ, and η_L of 2-propanol and acetone at or close to saturation conditions over a broad T range provide a valuable extension of the current data situation for these properties. The results can be considered as a reliable data source for future improvement of appropriate reference correlations and databases.

Supplementary Information The online version contains supplementary material available at https://doi.org/10.1007/s10765-023-03294-z.

Acknowledgements The authors gratefully acknowledge funding of the Erlangen Graduate School in Advanced Optical Technologies by the Bavarian State Ministry for Science and Art.

Author Contributions MK, JHJ, and APF contributed to the study conception and design. Experimental investigations and evaluations were performed by LMB, MK, and JHJ. The first draft of the manuscript was written by MK. All authors reviewed the manuscript and approved the final version.

Funding Open Access funding enabled and organized by Projekt DEAL. This work was funded by the Bavarian Ministry of Economic Affairs, Regional Development and Energy.

Declarations

Competing interest The authors declare they have no competing interests as defined by Springer, or other interests that might be perceived to influence the results and/or discussion reported in this paper.

References

1. A.N.A. Aryee, B.K. Simpson, J. Food Eng. **92**, 353 (2009). https://doi.org/10.1016/j.jfoodeng.2008.12.011
2. C. Garcia-Viguera, P. Zafrilla, F.A. Tomás-Barberán, Phytochem. Anal. **9**, 274 (1998). https://doi.org/10.1002/(SICI)1099-1565(199811/12)9:6%3c274::AID-PCA416%3e3.0.CO;2-G
3. Z. Liu, F.-S. Zhang, Energy Convers. Manag. **49**, 3498 (2008). https://doi.org/10.1016/j.enconman.2008.08.009
4. F.L. Mota, A.P. Carneiro, A.J. Queimada, S.P. Pinho, E.A. Macedo, Eur. J. Pharm. Sci. **37**, 499 (2009). https://doi.org/10.1016/j.ejps.2009.04.009
5. S.-J. Park, S.-Y. Jeon, S.-D. Yeo, Ind. Eng. Chem. Res. **45**, 2287 (2006). https://doi.org/10.1021/ie0510775
6. A. Proctor, D.J. Bowen, J. Am. Oil Chem. Soc. **73**, 811 (1996). https://doi.org/10.1007/BF02517960
7. S.A. Torabi, F.S. Choukami, I. Nikkhah, G. Khayati, Ind. Eng. Chem. Res. **62**, 7975 (2023). https://doi.org/10.1021/acs.iecr.3c00154
8. Y. Alhassan, N. Kumar, I.M. Bugaje, H.S. Pali, P. Kathkar, Energy Convers. Manag. **84**, 640 (2014). https://doi.org/10.1016/j.enconman.2014.04.080
9. T. Komanoya, K. Nakajima, M. Kitano, M. Hara, J. Phys. Chem. C **119**, 26540 (2015). https://doi.org/10.1021/acs.jpcc.5b08355

10. Y.-S. Huang, K. Sundmacher, Int. J. Chem. Kinet. **39**, 245 (2007). https://doi.org/10.1002/kin.20236
11. J. Klabunde, C. Bischoff, A.J. Papa, *Propanols*, in *Ullmann's Encycl. Ind. Chem.* (Wiley, Weinheim, 2018), pp. 1–14. https://doi.org/10.1002/14356007.a22_173.pub3
12. K. Jeřábek, J. Odnoha, K. Setínek, Appl. Catal. **37**, 129 (1988). https://doi.org/10.1016/S0166-9834(00)80756-3
13. Y.Z. Chen, C.M. Hwang, C.W. Liaw, Appl. Catal. A **169**, 207 (1998). https://doi.org/10.1016/S0926-860X(98)00019-2
14. V. Chikán, Á. Molnár, K. Balázsik, J. Catal. **184**, 134 (1999). https://doi.org/10.1006/jcat.1999.2437
15. M.J.D. Mahboub, J.-L. Dubois, F. Cavani, M. Rostamizadeh, G.S. Patience, Chem. Soc. Rev. **47**, 7703 (2018). https://doi.org/10.1039/C8CS00117K
16. A. Keskin, M. Gürü, Energy Sources Part A **33**, 2194 (2011). https://doi.org/10.1080/15567030903530558
17. A. Elfasakhany, Eng. Sci. Technol. Int. J. **19**, 1224 (2016). https://doi.org/10.1016/j.jestch.2016.02.002
18. N.H. Kasmuri, S.K. Kamarudin, S.R.S. Abdullah, H.A. Hasan, A.M. Som, Renew. Sustain. Energy Rev. **79**, 914 (2017). https://doi.org/10.1016/j.rser.2017.05.182
19. D.J. Gaspar, *Top Ten Blendstocks for Turbocharged Gasoline Engines: Bio-Blendstocks with Potential to Deliver the Highest Engine Efficiency* (Richland, WA, 2019). https://doi.org/10.2172/1567705
20. D. Cao, S.H. Bergens, J. Power. Sources **124**, 12 (2003). https://doi.org/10.1016/S0378-7753(03)00613-X
21. Z. Qi, J. Power. Sources **112**, 121 (2002). https://doi.org/10.1016/S0378-7753(02)00357-9
22. A. Anis, S.M. Al-Zahrani, F.A.A. El Aleem, Int. J. Electrochem. Sci. **7**, 6221 (2012). https://doi.org/10.1016/S1452-3981(23)19476-4
23. M. Brodt, K. Müller, J. Kerres, I. Katsounaros, K. Mayrhofer, P. Preuster, P. Wasserscheid, S. Thiele, Energy Technol. **9**, 4 (2021). https://doi.org/10.1002/ente.202100164
24. B.A. Santasalo, T. Kallio, K. Kontturi, Platin. Met. Rev. **53**, 58 (2009). https://doi.org/10.1595/147106709X416040
25. S.S. Gupta, J. Datta, J. Chem. Sci. **117**, 337 (2005). https://doi.org/10.1007/BF02708448
26. N. Kariya, A. Fukuoka, M. Ichikawa, Phys. Chem. Chem. Phys. **8**, 1724 (2006). https://doi.org/10.1039/b518369c
27. G. Sievi, D. Geburtig, T. Skeledzic, A. Bösmann, P. Preuster, O. Brummel, F. Waidhas, M.A. Montero, P. Khanipour, I. Katsounaros, J. Libuda, K.J.J. Mayrhofer, P. Wasserscheid, Energy Environ. Sci. **12**, 2305 (2019). https://doi.org/10.1039/C9EE01324E
28. P. Hauenstein, D. Seeberger, P. Wasserscheid, S. Thiele, Electrochem. Commun. **118**, 106786 (2020). https://doi.org/10.1016/j.elecom.2020.106786
29. J. Cho, B. Kim, S. Venkateshalu, D.Y. Chung, K. Lee, S.-I. Choi, J. Am. Chem. Soc. **145**, 16951 (2023). https://doi.org/10.1021/jacs.2c13324
30. F.J.V. Santos, C.A. Nieto de Castro, J.H. Dymond, N.K. Dalaouti, M.J. Assael, A. Nagashima, J. Phys. Chem. Ref. Data **35**, 1 (2006). https://doi.org/10.1063/1.1928233
31. C.A. Nieto de Castro, F.J.V. Santos, J.M.N.A. Fareleira, W.A. Wakeham, J. Chem. Eng. Data **54**, 171 (2009). https://doi.org/10.1021/je800528e
32. G. Scalabrin, P. Stringari, J. Phys. Chem. Ref. Data **38**, 127 (2009). https://doi.org/10.1063/1.3112608
33. M. Gude, A.S. Teja, J. Chem. Eng. Data **40**, 1025 (1995). https://doi.org/10.1021/je00021a001
34. E.W. Lemmon, I.H. Bell, M.L. Huber, M.O. McLinden, (2018). https://doi.org/10.18434/T4/1502528
35. P.S. Schmidt, M. Kerscher, T. Klein, J.H. Jander, F.E. Berger Bioucas, T. Rüde, S. Li, M. Stadelmaier, S. Hanyon, R.R. Fathalla, A. Bösmann, P. Preuster, P. Wasserscheid, T.M. Koller, M.H. Rausch, A.P. Fröba, Int. J. Hydrogen Energy **47**, 6111 (2022). https://doi.org/10.1016/j.ijhydene.2021.11.198
36. J.H. Jander, P.S. Schmidt, C. Giraudet, P. Wasserscheid, M.H. Rausch, A.P. Fröba, Int. J. Hydrogen Energy **46**, 19446 (2021). https://doi.org/10.1016/j.ijhydene.2021.03.093
37. E.H. Lucassen-Reynders, J. Lucassen, Adv. Colloid Interface Sci. **2**, 347 (1970). https://doi.org/10.1016/0001-8686(70)80001-X
38. D. Langevin, *Light Scattering by Liquid Surfaces and Complementary Techniques* (Dekker Marcel, New York, 1992)
39. A.P. Fröba, A. Leipertz, Int. J. Thermophys. **24**, 895 (2003). https://doi.org/10.1023/A:1025097311041

40. A.P. Fröba, *Simultane Bestimmung von Viskosität und Oberflächenspannung transparenter Fluide mittels Oberflächenlichtstreuung*, Dr.-Ing. Thesis. Friedrich-Alexander-Universität Erlangen-Nürnberg, 2002
41. A.P. Fröba, S. Will, Light Scattering by Surface Waves – Surface Light Scattering, in *Experimental Thermodynamics, Volume IX: Advances in Transport Properties of Fluids*. ed. by M.J. Assael, A.R.H. Goodwin, V. Vesovic, W.A. Wakeham (Royal Society of Chemistry, Cambridge, 2014), pp.19–74. https://doi.org/10.1039/9781782625254-00019
42. T.M. Koller, M. Kerscher, A.P. Fröba, J. Colloid Interface Sci. **626**, 899 (2022). https://doi.org/10.1016/j.jcis.2022.06.129
43. M. Kerscher, T. Klein, P.S. Schulz, E. Veroutis, S. Dürr, P. Preuster, T.M. Koller, M.H. Rausch, I.G. Economou, P. Wasserscheid, A.P. Fröba, Int. J. Hydrogen Energy **45**, 28903 (2020). https://doi.org/10.1016/j.ijhydene.2020.07.261
44. M. Kerscher, J.H. Jander, J. Cui, M.M. Martin, M. Wolf, P. Preuster, M.H. Rausch, P. Wasserscheid, T.M. Koller, A.P. Fröba, Int. J. Hydrogen Energy **47**, 15789 (2022). https://doi.org/10.1016/j.ijhydene.2022.03.051
45. M. Kerscher, A.P. Fröba, T.M. Koller, Int. J. Thermophys. **42**, 159 (2021). https://doi.org/10.1007/s10765-021-02909-7
46. J.H. Jander, M. Kerscher, J. Cui, J. Wicklein, T. Rüde, P. Preuster, M.H. Rausch, P. Wasserscheid, T.M. Koller, A.P. Fröba, Int. J. Hydrogen Energy **47**, 22078 (2022). https://doi.org/10.1016/j.ijhydene.2022.04.275
47. E.W. Lemmon, R. Span, J. Chem. Eng. Data **51**, 785 (2006). https://doi.org/10.1021/je050186n
48. M.L. Huber, *Models for Viscosity, Thermal Conductivity, and Surface Tension of Selected Pure Fluids as Implemented in REFPROP V10.0* (Gaithersburg, MD, 2018). https://doi.org/10.6028/NIST.IR.8209
49. K. Lucas, M. Luckas, *Berechnungsmethoden für Stoffeigenschaften, in VDI-Wärmeatlas* (Verein Deutscher Ingenieure, Düsseldorf, 1984)
50. B.E. Poling, J.M. Prausnitz, J.P. O'Connell, *The Properties of Gases and Liquids*, Fifth Edit (New York, 2001). https://doi.org/10.1036/0070116822
51. D.O. Ortiz Vega, K.R. Hall, J.C. Holste, A.H. Harvey, E.W. Lemmon, *An Equation of State for the Thermodynamic Properties of Helium* (Gaithersburg, MD, 2023). https://doi.org/10.6028/NIST.IR.8474
52. T.M. Koller, T. Klein, C. Giraudet, J. Chen, A. Kalantar, G.P. van der Laan, M.H. Rausch, A.P. Fröba, J. Chem. Eng. Data **62**, 3319 (2017). https://doi.org/10.1021/acs.jced.7b00363
53. T. Klein, F.D. Lenahan, M. Kerscher, M.H. Rausch, I.G. Economou, T.M. Koller, A.P. Fröba, J. Phys. Chem. B **124**, 4146 (2020). https://doi.org/10.1021/acs.jpcb.0c01740
54. M. Kerscher, J.H. Jander, F. Luther, P. Schühle, M. Richter, M.H. Rausch, A.P. Fröba, Int. J. Hydrogen Energy **48**, 26817 (2023). https://doi.org/10.1016/j.ijhydene.2023.03.312
55. J. Cui, M. Kerscher, J.H. Jander, T. Rüde, P.S. Schulz, P. Wasserscheid, M.H. Rausch, T.M. Koller, A.P. Fröba, J. Chem. Eng. Data **67**, 3085 (2022). https://doi.org/10.1021/acs.jced.2c00519
56. A. Mulero, I. Cachadiña, E.L. Sanjuán, J. Phys. Chem. Ref. Data **44**, 033104 (2015). https://doi.org/10.1063/1.4927858
57. A. Mulero, I. Cachadiña, M.I. Parra, J. Phys. Chem. Ref. Data **41**, 043105 (2012). https://doi.org/10.1063/1.4768782
58. G. Vazquez, E. Alvarez, J.M. Navaza, J. Chem. Eng. Data **40**, 611 (1995). https://doi.org/10.1021/je00019a016
59. S. Azizian, N. Bashavard, J. Chem. Eng. Data **50**, 1303 (2005). https://doi.org/10.1021/je0500431
60. Y.-C. Kao, C.-H. Tu, J. Chem. Thermodyn. **43**, 216 (2011). https://doi.org/10.1016/j.jct.2010.08.019
61. A.E. Andreatta, E. Rodil, A. Arce, A. Soto, J. Solut. Chem. **43**, 404 (2014). https://doi.org/10.1007/s10953-014-0128-9
62. C.-W. Chang, T.-L. Hsiung, C.-P. Lui, C.-H. Tu, Fluid Phase Equilib. **389**, 28 (2015). https://doi.org/10.1016/j.fluid.2014.12.040
63. A.I. Vogel, J. Chem. Soc. **1**, 1814 (1948). https://doi.org/10.1039/jr9480001814
64. H. Ghahremani, A. Moradi, J. Abedini-Torghabeh, S.M. Hassani, Der Chem. Sin. **2**, 212 (2011)
65. J.L. Pérez-Díaz, M.A. Álvarez-Valenzuela, J.C. García-Prada, J. Colloid Interface Sci. **381**, 180 (2012). https://doi.org/10.1016/j.jcis.2012.05.034
66. R.P. Worley, J. Chem. Soc. Trans. **105**, 273 (1914). https://doi.org/10.1039/CT9140500273
67. T. Tonomura, K. Chujo, Bull. Chem. Soc. Jpn **7**, 259 (1932). https://doi.org/10.1246/bcsj.7.259

68. D.M. Cowan, G.H. Jeffery, A.I. Vogel, J. Chem. Soc. **171**, 75 (1940). https://doi.org/10.1039/jr9400000171
69. J.L.R. Morgan, A.J. Scarlett, J. Am. Chem. Soc. **39**, 2275 (1917). https://doi.org/10.1021/ja02256a003
70. A.I. Toryanik, V.G. Porebnyak, J. Struct. Chem. **17**, 464 (1977). https://doi.org/10.1007/BF00746671
71. R.A. Stairs, W.T. Rispin, R.C. Makhija, Can. J. Chem. **48**, 2755 (1970). https://doi.org/10.1139/v70-464
72. H. Kahl, T. Wadewitz, J. Winkelmann, J. Chem. Eng. Data **48**, 580 (2003). https://doi.org/10.1021/je0201323
73. S. Enders, H. Kahl, J. Winkelmann, J. Chem. Eng. Data **52**, 1072 (2007). https://doi.org/10.1021/je7000182
74. T.E. Thorpe, J.W. Rodger, Proc. R. Soc. Lond. **60**, 152 (1897). https://doi.org/10.1098/rspl.1896.0026
75. S. Aznarez, A. Amid, M.M.E.F. de Ruiz Holgado, E.L. Arancibia, J. Mol. Liq. **115**, 69 (2004). https://doi.org/10.1016/j.molliq.2004.04.002
76. C. Yang, H. Lai, Z. Liu, P. Ma, J. Chem. Eng. Data **51**, 584 (2006). https://doi.org/10.1021/je050414d
77. F.-M. Pang, C.-E. Seng, T.-T. Teng, M.H. Ibrahim, J. Mol. Liq. **136**, 71 (2007). https://doi.org/10.1016/j.molliq.2007.01.003
78. A.M. Awwad, H.A. Alsyouri, K.A. Jbara, J. Chem. Eng. Data **53**, 1655 (2008). https://doi.org/10.1021/je8003194
79. F. Kermanpour, T. Sharifi, J. Chem. Eng. Data **59**, 1922 (2014). https://doi.org/10.1021/je401101u
80. F.M.R. Mesquita, F.X. Feitosa, M. Aznar, H.B. de Santana, R.S. Santiago-Aguiar, J. Chem. Eng. Data **59**, 2196 (2014). https://doi.org/10.1021/je500153g
81. S.G. Shirazi, F. Kermanpour, J. Chem. Eng. Data **64**, 2292 (2019). https://doi.org/10.1021/acs.jced.8b01097
82. W. Weber, Rheol. Acta **14**, 1012 (1975). https://doi.org/10.1007/BF01516304
83. K.S. Howard, R.A. McAllister, AIChE J. **4**, 362 (1958). https://doi.org/10.1002/aic.690040326
84. T. Ling, M. van Winkle (1958) Ind. Eng. Chem. Chem. Eng. Data Ser. **3**, 88 https://doi.org/10.1021/i460003a018
85. M. Hafez, S. Hartland, J. Chem. Eng. Data **21**, 179 (1976). https://doi.org/10.1021/je60069a011
86. S. Govindarajan, V. Kannappan, M.D. Naresh, K. Venkataboopathy, B. Lokanadam, J. Mol. Liq. **107**, 289 (2003). https://doi.org/10.1016/S0167-7322(03)00156-9
87. I.-H. Peng, C.-H. Tu, J. Chem. Eng. Data **47**, 1457 (2002). https://doi.org/10.1021/je020077y
88. H.-W. Chen, C.-H. Tu, J. Chem. Eng. Data **50**, 1262 (2005). https://doi.org/10.1021/je0500101
89. L. Yang, T. Luo, H. Lian, G. Liu, J. Chem. Eng. Data **55**, 1364 (2010). https://doi.org/10.1021/je900535d
90. R. Sih, M. Armenti, R. Mammucari, F. Dehghani, N. R. Foster **43**, 460 (2008). https://doi.org/10.1016/j.supflu.2007.08.001
91. O. Faust, Zeitschrift Für Phys. Chemie **79U**, 97 (1912). https://doi.org/10.1515/zpch-1912-7906

Authors and Affiliations

Manuel Kerscher[1] · Lena M. Braun[1] · Julius H. Jander[1] · Michael H. Rausch[1] · Thomas M. Koller[1] · Peter Wasserscheid[2,3] · Andreas P. Fröba[1]

✉ Andreas P. Fröba
andreas.p.froeba@fau.de

Manuel Kerscher
manuel.kerscher@fau.de

Lena M. Braun
lena.br.braun@fau.de

Julius H. Jander
julius.jander@fau.de

Michael H. Rausch
michael.rausch@fau.de

Thomas M. Koller
thomas.m.koller@fau.de

Peter Wasserscheid
peter.wasserscheid@fau.de

[1] Institute of Advanced Optical Technologies – Thermophysical Properties (AOT-TP), Department of Chemical and Biological Engineering (CBI) and Erlangen Graduate School in Advanced Optical Technologies (SAOT), Friedrich-Alexander-Universität Erlangen-Nürnberg (FAU), Paul-Gordan-Straße 8, 91052 Erlangen, Germany

[2] Forschungszentrum Jülich GmbH, Helmholtz Institute Erlangen-Nürnberg for Renewable Energy (IEK-11), Cauerstraße 1, 91058 Erlangen, Germany

[3] Institute of Chemical Reaction Engineering (CRT), Department of Chemical and Biological Engineering (CBI), Friedrich-Alexander-Universität Erlangen-Nürnberg (FAU), Egerlandstraße 3, 91058 Erlangen, Germany